



Article

Research on Polar Operational Limit Assessment Risk Indexing System for Ships Operating in Seasonal Sea-Ice Covered Waters

Jin Xu ^{1,2,3,4} , Shuai Xu ¹, Long Ma ^{1,2,3,4,*}, Sihan Qian ^{1,4}  and Xiaowen Li ²

¹ Naval Architecture and Shipping College, Guangdong Ocean University, Zhanjiang 524088, China; jinxu@gdou.edu.cn (J.X.); xs20221053@163.com (S.X.); 18861913315@stu.gdou.edu.cn (S.Q.)

² Key Laboratory of Philosophy and Social Science in Hainan Province of Hainan Free Trade Port International Shipping Development and Property Digitization, Hainan Vocational University of Science and Technology, Haikou 570100, China; xiaowenli_capt@126.com

³ Guangdong Provincial Engineering Research Center for Ship Intelligence and Safety, Guangdong Ocean University, Zhanjiang 524088, China

⁴ Guangdong Provincial Key Laboratory of Intelligent Equipment for South China Sea Marine Ranching, Guangdong Ocean University, Zhanjiang 524088, China

* Correspondence: malong@gdou.edu.cn

Abstract: The Polar Operational Limit Assessment Risk Indexing System (POLARIS) has been established as a viable framework for assessing operational capabilities and associated risks in polar waters. Despite its inherent suitability for high-latitude territories, ships navigating through seasonal ice-infested waters at lower latitudes also encounter critical safety, environmental, and economic issues exacerbated by the presence of ice. This necessitates a reliable and adaptable methodology that can serve as a reference for devising effective countermeasures. This study evaluated the use of POLARIS in the intricate ice conditions prevalent in the northern navigable waters (channels and anchorages) within Liaodong Bay of the Bohai Sea, located at relatively low latitudes. Using GF-4 satellite imagery, ice conditions were collected, and the POLARIS methodology was employed to calculate Risk Index Outcome (RIO) values for non-ice-strengthened vessels during the winter season of 2021–2022. The results showed that sectors 3, 4, 5, 7, 9, 10, and 11 within the northern part of Liaodong Bay exhibited a higher risk, with sectors 5 and 10 exhibiting the most significant risk, while sectors 1 and 2 demonstrated relatively lower risk levels. The concurrence of these findings with acknowledged ice patterns and local maritime practices confirms the applicability of the POLARIS methodology in saline, seasonally ice-covered seas. Notably, the combination of POLARIS with high-resolution satellite imagery facilitated a more precise and rapid assessment of ice risk, thereby enhancing situational awareness and informing decision-making processes in maritime operations under icy conditions. In addition, this study provides preliminary evidence that POLARIS is suitable for fine-scale scenarios, in addition to being applicable to sparse-scale scenarios, such as polar waters, especially with high-resolution ice data. At the same time, this study highlights the potential of POLARIS as a disaster prevention strategy and a tool for the maritime industry to address ice challenges.

Keywords: POLARIS; navigable waters; sea ice thickness; maritime safety



Citation: Xu, J.; Xu, S.; Ma, L.; Qian, S.; Li, X. Research on Polar Operational Limit Assessment Risk Indexing System for Ships Operating in Seasonal Sea-Ice Covered Waters. *J. Mar. Sci. Eng.* **2024**, *12*, 827. <https://doi.org/10.3390/jmse12050827>

Academic Editor: Anatoly Gusev

Received: 18 April 2024

Revised: 13 May 2024

Accepted: 13 May 2024

Published: 16 May 2024



Copyright: © 2024 by the authors. Licensee MDPI, Basel, Switzerland. This article is an open access article distributed under the terms and conditions of the Creative Commons Attribution (CC BY) license (<https://creativecommons.org/licenses/by/4.0/>).

1. Introduction

The Bohai Sea, being the northernmost inland sea in China and one of the lowest latitude regions globally where sea ice formation occurs [1,2], experiences varying degrees of icing conditions annually due to the intrusion of cold air masses sweeping down from higher latitudes. This annual ice season, lasting approximately three months between December and February, not only shapes the regional climate dynamics but also directly impacts numerous economic sectors relying on marine access and operations. Vessel navigation, port activities, offshore oil and gas exploration, aquaculture industries, and other

maritime-dependent businesses face intermittent disruptions and heightened operational challenges resulting from the unpredictable and often harsh ice conditions [2–4]. The 2021 China Marine Disaster Bulletin emphasized the severity of these challenges, reporting mean direct economic losses exceeding 102.70 million yuan (approximately 15.86 million USD) over the last decade alone, attributed to sea ice-related disasters [5].

In response to the pressing need for better risk management in these ice-infested environments, stakeholders ranging from government regulators to maritime service providers are seeking reliable methods to accurately evaluate and mitigate risks. The POLARIS, supported by the International Maritime Organization (IMO), has emerged as a promising instrument for quantifying such risks in polar waters and is receiving attention from both academic researchers and the global shipping industry. Fedi et al.'s critical appraisal of POLARIS [6] underscored its multifaceted utility: they noted that the Polar Code recommends the use of POLARIS by shipowners and classification societies to determine the necessary ice strengthening requirements for vessels—a recommendation corroborated by empirical evidence presented by Kujala et al. [7]. Insurers are advised to consult POLARIS when evaluating a ship's vulnerability to ice entrapment and structural damage; and insurance premium calculations can be grounded in the risk assessment outputs derived from POLARIS. Bond et al. emphasize that with POLARIS, one can utilize historical ice data for voyage planning, incorporate forecasted ice for short-term course plotting, and make immediate decisions at the bridge based on the impending ice conditions [8]. Additionally, Fedi et al.'s investigation into accidents reinforced the notion that integrating the Polar Code with POLARIS is a sound approach to reducing the level of risk in polar contexts [9].

While POLARIS is predominantly applied in polar environments, its design meticulously accounts for a vessel's structural resistance to ice loads and the resilience of its propulsion and steering systems under icy conditions, as well as prevailing ice regimes, to evaluate operational risks. This design framework indicates POLARIS's potential applicability to icy regions beyond the polar zones. Indeed, researchers have initiated limited explorations into employing POLARIS in seasonally ice-covered waters. For instance, Tremblet's preliminary study in the Great Lakes highlighted that while POLARIS guidelines largely align with safe shipping practices in these freshwater systems, it also pinpointed the importance of considering the distinct characteristics of freshwater lake ice [10]. Moakler et al. developed a freshwater adaptation of POLARIS and proposed that freshwater ice zones, such as the Great Lakes or the Bohai Sea, should undergo validation [11]. It should be noted that, according to the measured data, the average salinity in the Bohai Sea exceeds 30 parts per thousand (ppt) [12], while most of the ocean has a salinity ranging between 34 parts per thousand (ppt) and 36 ppt. As a result, the Bohai Sea, with its distinctive features of high salinity and seasonal icing, offers a fresh perspective for validating and refining the POLARIS methodology.

This study focused on the adaptability of POLARIS methodology for assessing operational risks facing vessels operating in saline, seasonal sea-ice covered waters, taking the northern navigable waters (including channels and anchorages) of Liaodong Bay as an example—a critical area within the Bohai Sea known for experiencing the harshest ice conditions [1]. By employing POLARIS, we utilized RIO values to systematically identify navigable sectors that present considerable safety threats to non-ice-strengthened vessels. This study not only examined the practical relevance of POLARIS in this unique seasonal ice environment based on the collective expertise and operational strategies of maritime professionals, but also demonstrated how the application of RIO in ice-infested voyages can significantly improve situational awareness of winter-season hazards. Furthermore, employing high-resolution GF-4 satellite imagery to capture ice conditions within the study area, POLARIS has enabled the assessment of operational risks confronting vessels in small-scale ice-infested waters, thereby making it feasible to evaluate ice-related risks to ships directly from the bridge and extending the application of POLARIS.

2. Study Area and Data

2.1. Study Area

The navigable waters in the northern part of Liaodong Bay, including channels and anchorages at Huludao, Jinzhou, Panjin, and Yingkou ports, are significantly impacted by sea ice, as detailed in Figure 1 and Table 1. In this figure, numerals 1 through 12 (indicated in black) correspond to entries 1 through 12 in the table. Notably, numeral 13 represents the northern waters of Liaodong Bay (light-grey area), with its southern boundary defined by pilot boarding points at each of these ports. The geographical locations listed in the table have been sourced from electronic nautical charts, the chinaports website, and the ‘China Sailing Directions A101’ published in 2006.

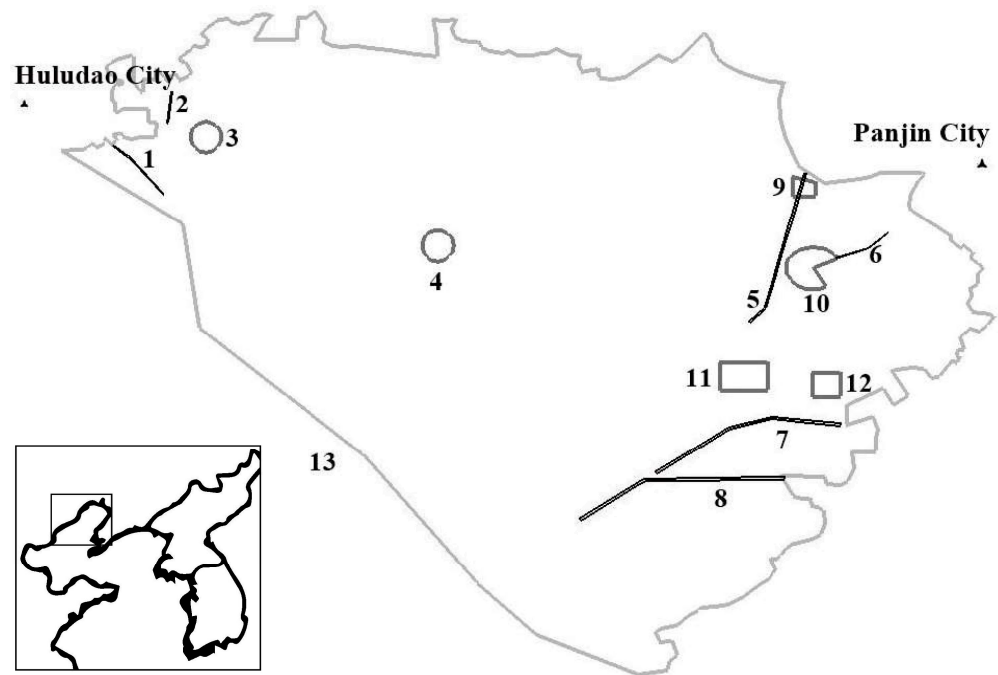


Figure 1. Navigable waters and northern waters of Liaodong Bay.

Table 1. Navigable waters of the northern Liaodong Bay.

No.	Navigable Waters	Geographic Locations
1	Huludao main channel	From Huludao No. 1 light buoy (40°37'30" N, 121°02'55" E) to No. 16 light buoy
2	Jinzhou Gang main channel	From Jinzhou Gang No. 1 light buoy (40°43'29" N, 121°03'12" E) to No. 7 light buoy
3	Jinzhou Gang No. 1 anchorage	Centered at 40°42'24" N, 121°06'30" E, radius 1 nm
4	Jinzhou Gang No. 2 anchorage	Centered at 40°33'00" N, 121°26'30" E, radius 1 nm
5	Main channel of Rongxing harbor area of Yingkou Gang	From Panjin Gang No. 1 light buoy (40°26'26" N, 121°53'35" E) to No. 35 light buoy
6	Channel of Yingkou harbor area of Yingkou Gang	From Yingkou harbor area No. 1 light buoy (40°31'54" N, 122°01'00" E) to No. 11 light buoy
7	Channel of Bayuquan harbor area of Yingkou Gang	From Bayuquan harbor area No. 1 light buoy (40°13'22" N, 121°45'30" E) to No. 36 light buoy

Table 1. *Cont.*

No.	Navigable Waters	Geographic Locations
8	Channel of Xianrendao harbor area of Yingkou Gang	From Xianrendao harbor area No. 1 light buoy (40°09'19" N, 121°38'59" E) to No. 40 light buoy
9	Transshipment anchorage	121°57'09" E 40°37'17" N 121°59'08" E 40°37'17" N 121°59'08" E 40°38'34" N 121°57'09" E 40°39'01" N Anchorage connected by the above four points
10	Quarantine anchorage	Centered at Yingkou Light Float (40°31'06" N, 121°58'58" E), radius 1.8 nm. A 3/4 circle formed by rotating 270° anticlockwise from Yingkou Light Float to No. 1 light buoy as the starting edge
11	Large vessels anchorage	121°55'03" E 40°22'55" N 122°50'51" E 40°22'55" N 121°50'51" E 40°20'31" N 122°55'03" E 40°20'31" N Anchorage connected by the above four points
12	Small vessels anchorage	121°58'51" E 40°20'01" N 122°01'21" E 40°20'01" N 122°01'21" E 40°22'01" N 121°58'51" E 40°22'01" N Anchorage connected by the above four points

2.2. Data

High-resolution imagery from the GF-4 satellite was employed to obtain ice condition data for POLARIS, complemented by temperature readings from the Yingkou weather station to analyze operational risks in ice-infested areas.

2.2.1. Remote Sensing Data

The GF-4 satellite, launched on 29 December 2015, hosts a camera able to capture 50 m resolution visible–near infrared imagery and 400 m resolution mid-wave infrared imagery, enabling full coverage of the study area in one shot. Utilizing these visible–near infrared bands, an estimation of the sea ice thickness in the northern part of Liaodong Bay has been conducted, with specific parameters provided in Table 2, where Band 1 refers to the panchromatic band.

Table 2. Parameters of VIS/NIR bands.

Band No.	Spectrum (μm)	Spatial Resolution (m)	Swath Width (km)	Revisit Period (s)
1	0.45~0.90			
2	0.45~0.52			
3	0.52~0.60	50	400	20
4	0.63~0.69			
5	0.76~0.90			

According to satellite observations, the sea ice freeze date in the Liaodong Bay during the 2021–2022 season was 17 December 2021, while the sea ice free date was 4 March 2022, thus yielding a total freezing duration of 78 days. Throughout this interval, there were 44 days with clear skies, and correspondingly, 44 cloud-free images were obtained for the study area.

2.2.2. Temperature Data

In this study, daily mean temperature records collected by the Yingkou meteorological station between 17 December 2021 and 4 March 2022, were retrieved. Previous research demonstrated a significant correlation between sea ice development and accumulated temperature [1,13]. Figure 2 illustrates the accumulated temperature at the Yingkou meteorological station, distinctly showing a turning point on February 24th when the accumulated temperature started to reverse its course.

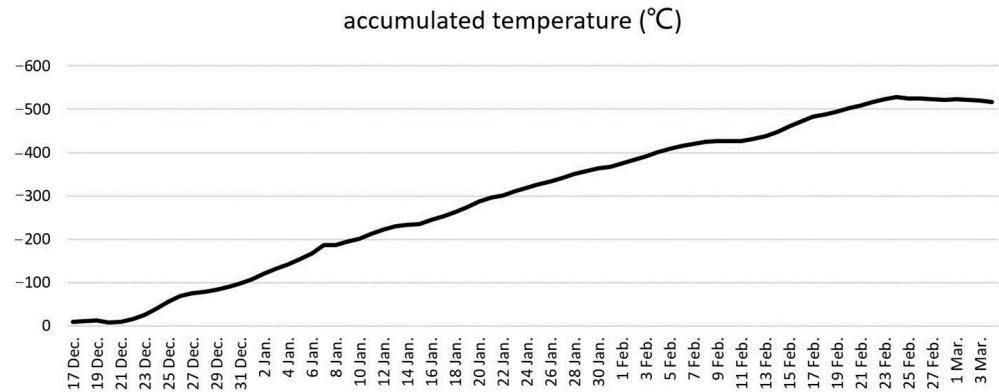


Figure 2. Accumulated temperature of the freezing stage at Yingkou weather station.

3. Methodology and Analysis Logic

3.1. Methodology [14]

POLARIS employs a RIO value to assess limitations for operation in ice-covered waters. Specifically, Risk Index Values (RIVs) are allotted to vessels in accordance with their ice class and the types of ice encountered within navigational routes, as outlined in Table 3. The RIO value is subsequently calculated through the summation of RIVs corresponding to each ice type present in the prevailing ice regime, with each RIV being multiplied by the concentration of that ice type, expressed in tenths:

$$RIO = (C_1 \times RIV_1) + (C_2 \times RIV_2) + (C_3 \times RIV_3) + \dots + (C_n \times RIV_n) \quad (1)$$

where $C_1 \dots C_n$ are the concentrations (in tenths) of ice types within the ice regime, and $RIV_1 \dots RIV_n$ are the corresponding Risk Index Values for each ice type.

Table 3. Risk Index Values.

Ice Class	Ice-Free	New Ice	Gray Ice	Gray White Ice	Thin First Year Ice 1st Stage	Thin First Year Ice 2st Stage	Medium First Year Ice Less than 1 m Thick	Medium First Year Ice	Thick First Year Ice	Second Year Ice	Light Multi Year Ice, Less than 2.5 m Thick	Heavy Multi Year Ice
PC1	3	3	3	3	2	2	2	2	2	2	1	1
PC2	3	3	3	3	2	2	2	2	2	1	1	0
PC3	3	3	3	3	2	2	2	2	2	1	0	-1
PC4	3	3	3	3	2	2	2	2	1	0	-1	-2
PC5	3	3	3	3	2	2	1	1	0	-1	-2	-2
PC6	3	2	2	2	2	1	1	0	-1	-2	-3	-3
PC7	3	2	2	2	1	1	0	-1	-2	-3	-3	-3
IA Super	3	2	2	2	2	1	0	-1	-2	-3	-4	-4
IA	3	2	2	2	1	0	-1	-2	-3	-4	-5	-5
IB	3	2	2	1	0	-1	-2	-3	-4	-5	-6	-6
IC	3	2	1	0	-1	-2	-3	-4	-5	-6	-7	-8
Not Ice Strengthened	3	1	0	-1	-2	-3	-4	-5	-6	-7	-8	-8

Lower RIO values indicate higher risk, with differing RIO levels implying the necessity for different operational measures for the vessel (Table 4).

Table 4. Risk Index Outcome Criteria.

RIO _{ship}	Ice Classes PC1-PC7	Ice Classes below PC7 and Ships Not Assigned an Ice Class
RIO ≥ 0	Normal operation	Normal operation
−10 ≤ RIO < 0	Elevated operational risk	Operational subject to special consideration
RIO < −10	Operational subject to special consideration	Operational subject to special consideration

In seasonally ice-covered waters, the assigned RIVs for non-ice-strengthened vessels are referred to in Table 5. Regarding sea ice types, they inherently represent the sea ice thickness and can, therefore, be determined using the estimated sea ice thickness derived from satellite data.

Table 5. RIVs for non-ice-strengthened vessels.

Ice Class	Ice Free	New Ice	Gray Ice	Gray White Ice	Thin First Year Ice 1st Stage	Thin First Year Ice 2st Stage	Medium First Year Ice	Thick First Year Ice
Not Ice Strengthened	3	1	0	−1	−2	−3	−5	−6

For independently navigating vessels, the RIO is computed by multiplying the RIV with the local sea ice concentration (Equation (1)). Owing to the utilization of high-resolution GF-4 satellite imagery, pixels classified as encompassing sea ice are assumed to signify complete sea ice coverage, or 10/10 concentration. Therefore, in accordance with this assumption, the calculation of RIO entails multiplying the RIV by a factor of 10.

3.2. Analysis Logic

Figure 3 depicts the analysis logic employed in the present study, and the subsequent text provides a detailed description of its contents.

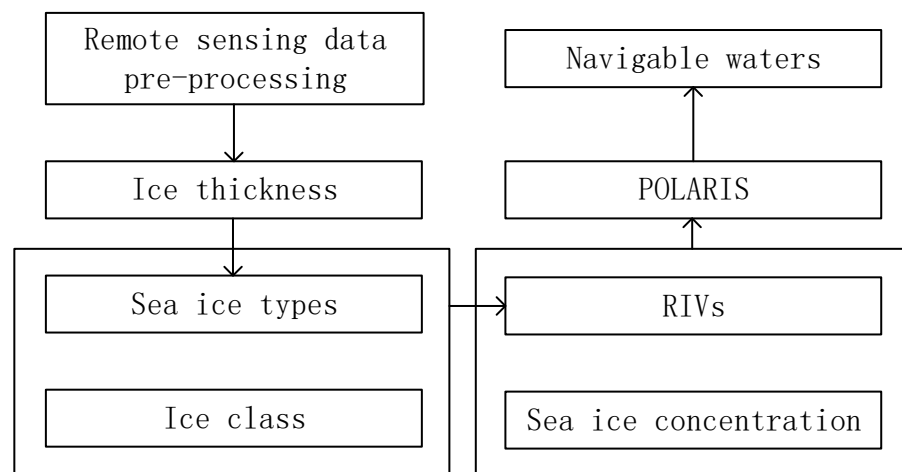


Figure 3. Analysis logic.

(1) Satellite remote sensing data preprocessing consisted of radiometric calibration and geometric correction. Following this, the estimation of sea ice thickness was performed (Figure 4), referencing the research work by Yuan [15,16].

Ice thickness in the study area on 21 January 2022

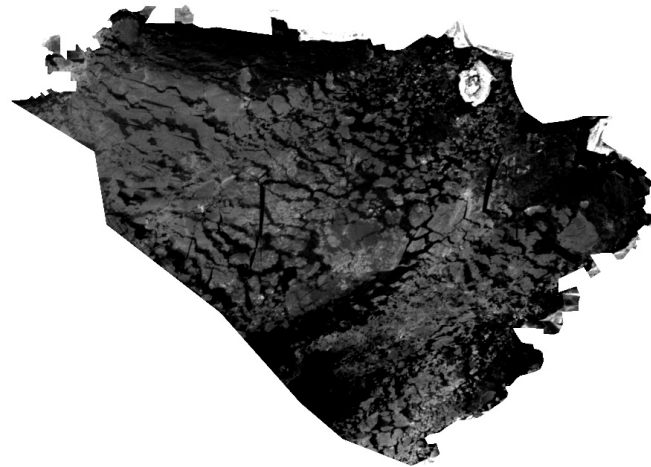


Figure 4. Example: Ice thickness in the study area on 21 January 2022.

(2) Based on the relationship between sea ice thickness and sea ice type, the sea ice types were derived by discretizing the estimated sea ice thickness and were subsequently verified by comparing them with the visually interpreted types in the original images. The results indicated a good match between the categorized sea ice types and those from visual interpretation.

(3) In this study, a fixed sea ice concentration value of 10 was applied. Leveraging the POLARIS methodology, the RIO values were calculated by multiplying the derived RIV with this constant value of 10. This method produced 44 distinct RIO maps covering the northern waters of Liaodong Bay throughout the 2021–2022 winter season.

(4) The vector data representing the 12 navigable regions within Figure 1 and listed in Table 1 were extracted and subsequently superimposed onto each of the 44 individual RIO maps (as depicted in Figure 5). By performing these overlay operations, the RIO values were computed specifically for the 12 navigable areas within the northern waters of Liaodong Bay.

RIO for the study area on 21 January 2022

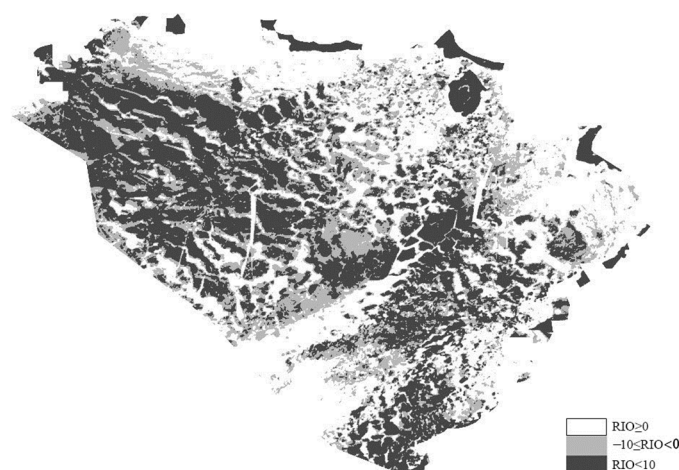


Figure 5. Example: RIO for the study area on 21 January 2022.

It was important to note that when calculating the RIO values, the process of discretizing sea ice thickness data and the subsequent segmentation process both considered the inherent uncertainty of ice information, which thereby ensured the reliability of the risk assessment results.

4. Results and Discussion

4.1. RIO Values of Navigable Waters

Table 6 presents the mean RIO values for the 44-day period across the navigable waters, alongside the percentage of days where the RIO value was either greater than or equal to zero ($RIO \geq 0$), between negative ten and zero ($-10 \leq RIO < 0$), and less than negative ten ($RIO < -10$). Furthermore, it documents the start and end dates of periods during which the RIO value fell below zero ($RIO < 0$) and below negative ten ($RIO < -10$), respectively. The duration between the start and end dates for instances when the RIO value was less than negative ten ($RIO < -10$) was defined in this context as the heavy ice period within the navigable waters. With regard to Table 6, the heavy ice period in navigable waters is mainly concentrated in January and February. According to the information provided by <https://globalmaritimetraffic.org/> (accessed on 10 May 2024), there is a significant reduction in traffic flow density during January and February, particularly in the northern waters of the Liaodong Bay.

Table 6. Statistics of RIO values for navigable waters.

Navigable Waters	Mean RIO	$RIO \geq 0$	$-10 \leq RIO < 0$	$RIO < -10$	Start Date of $RIO < 0$	End Date of $RIO < 0$	Start Date of $RIO < -10$	End Date of $RIO < -10$
1	9.68	77	14	9	Dec. 31	Feb. 23	Dec. 31	Feb. 2
2	7.03	70	12	18	Dec. 31	Feb. 15	Dec. 31	Feb. 1
3	2.42	41	36	23	Dec. 29	Feb. 23	Dec. 30	Feb. 4
4	3.43	41	36	23	Dec. 26	Feb. 23	Dec. 26	Feb. 16
5	-1.09	32	50	18	Dec. 26	Feb. 25	Jan. 11	Feb. 17
6	3.93	57	36	7	Dec. 26	Feb. 25	Dec. 29	Feb. 19
7	2.88	41	32	27	Dec. 27	Feb. 27	Jan. 20	Feb. 24
8	5.37	54	23	23	Jan. 19	Feb. 25	Jan. 19	Feb. 24
9	0.53	40	50	10	Dec. 26	Feb. 25	Dec. 28	Feb. 2
10	-1.43	36	41	23	Dec. 26	Feb. 27	Jan. 16	Feb. 24
11	1.72	43	34	23	Dec. 26	Feb. 25	Jan. 20	Feb. 24
12	5.05	52	21	27	Dec. 26	Feb. 23	Dec. 26	Feb. 21

It should be noted that the start and end dates for periods where the RIO value was less than zero ($RIO < 0$) and less than -10 ($RIO < -10$) indicate that before these specified dates or after them, no instances would occur where the RIO value dips below zero or -10 , respectively. However, within the time span between these start and end dates, there could be instances where the RIO value is observed to be either greater than or equal to zero ($RIO \geq 0$) or falling within the range between -10 and zero ($-10 \leq RIO < 0$).

The formation of sea ice in Liaodong Bay begins on coastal shoals and around the bay entrance, and it subsequently experiences redistribution driven by wind patterns and ocean currents, resulting in varying degrees of risk associated with ice conditions across the diverse navigable regions within the bay.

According to Table 6, the navigable waters 3, 4, 5, 7, 9, 10, and 11 exhibited relatively higher risks in terms of their mean RIO values and the proportion of days with RIO values less than zero. Among these, navigable waters 5 and 10 stood out with the highest risk levels, both featuring negative mean RIO values and the highest percentages of days where RIO was below zero—68% and 64%, respectively. The elevated risk in these two areas could be attributed to their close proximity to river estuaries, shallower water depths, and the impact of northwesterly winter monsoons, which together promoted a clustering of sea ice [17,18]. Additionally, navigable water 4 experienced the longest continuous period with RIO values less than -10 , essentially spanning the entire duration of satellite imaging. This extended period of severe ice conditions was largely due to the freshwater influx from rivers like the Liao River and the Daqing River into the northeastern section of Liaodong Bay, where lower salinity fostered increased sea ice formation. Notably, adjacent to navigable water 4 lies China’s most northern offshore oilfield cluster within its maritime boundaries, the China National Offshore Oil Corporation (CNOOC) Jinzhou 9-3 Oilfield Cluster.

Navigable waters 1 and 2 demonstrated a relatively lower risk, evidenced by earlier end dates for periods where RIO values dropped below -10 . This reduced risk might

stem from the combined influences of offshore winds [18], which tended to hinder sea ice accumulation, as well as tidal currents that further limited ice build-up. Additionally, during peak ice seasons, the residual warm current originating from the Yellow Sea and passing through the Bohai Strait exerted a substantial melting effect on sea ice along the western coast of Liaodong Bay [17]. Another point of interest is that navigable water 8 witnessed a later initiation of the heavy ice period, mainly due to its southerly position, which leads to a relatively delayed onset of sea ice formation.

4.2. Risks of Navigable Waters

In accordance with the POLARIS methodology, vessels navigating in these waters predominantly face the following risks:

(1) In navigable waters with relatively high risk (zones 3, 4, 7, 8, 9, 10, 11, and 12), where the proportion of days with RIO values less than zero ($\text{RIO} < 0$) is around 60% or higher, the risks include persistent sea ice conditions that significantly impede vessel operations, potentially leading to delays and damage.

(2) In waters exhibiting lower mean RIO values, especially navigable waters 5, 9, and 10, where the mean RIO values are close to or less than zero, the risks involve vast and thick layers of ice capable of inflicting considerable harm to vessels and disrupting port operations. A common scenario is when ports become inaccessible due to extreme ice conditions, necessitating ships to remain anchored or stranded for several days [19].

(3) Furthermore, particular vigilance should be directed toward navigable water 4. The ice conditions in this area present significant operational challenges to the platforms and guard vessels operating within the nearby CNOOC Jinzhou 9-3 offshore oilfield cluster.

Observations in this study area indicate that the winter of 2021–2022 was a normal ice year, while the subsequent two winters were classified as light ice years, exhibiting warm winter characteristics. The impact of sea ice in navigable waters on ship safety is likely to be generally small, but the development of sea ice may present rapid characteristics. Furthermore, temperature observations provided insights into the navigational risks. By comparing Figure 2 and Table 6, it could be discerned that after the turning point in cumulative temperatures occurred, the examined navigable waters also concluded their heavy ice period.

4.3. Applicability of the POLARIS Methodology

(1) Within the framework of the POLARIS methodology, gray white ice with a thickness ranging from 15 to 30 cm was assigned a RIO value of -1 for non-ice-strengthened vessels, necessitating special caution. In corroboration, Liu et al. emphasized that, in the Bohai Sea, once ice thickness surpasses 20 cm and its concentration exceeds 5/10, vessel safety becomes significantly challenged [20]. Additionally, Zhu's suggestions for vessel maneuvering in icy waters, particularly when the ice thickness surpasses 20 cm, involve methods such as squeezing through ice, crashing into ice, backing out along the same path, and accelerating in reverse [21]. These recommendations align with the POLARIS methodology's comprehension of the operational risks that vessels encounter.

(2) Annual winter reports addressing ice conditions or navigational hazards in the Liaodong Bay recurrently featured Panjin Port and Bayuquan Port [22], underscoring their positioning within the inland sections of the Liaodong Bay, where they are more susceptible to early and extensive ice formation [23]. Academic research indicates that single-layer ice thickness in the Liaodong Bay can reach up to 30–50 cm, with accumulated ice thickness reaching as much as 1–2 m [24]; moreover, the eastern waters experience a pronounced sea ice accumulation effect under the influence of winter winds [17]. These findings substantiate the high-risk navigable waters flagged by POLARIS, particularly referring to waters 5, 7, 9, 10, and 11.

(3) Navigable water 4 was also identified as a high-risk ice zone by the POLARIS methodology. This specific area has drawn notable media attention, with news articles focusing particularly on the Jinzhou 9-3 oilfield near navigable water 4 under headlines

such as “Ice-Breaking Operation: China’s Northernmost Offshore Oilfield’s Decades-long Struggle against Ice”. The report accentuated the substantial impact of sea ice on this oilfield situated adjacent to this navigable water.

In conclusion, this study confirms the effectiveness of the POLARIS methodology in identifying high-risk navigational zones for non-ice-strengthened vessels, thereby providing valuable guidance for mitigating risks in icy waters similar to those found in the Bohai Sea. Consequently, relevant government agencies and port/shipping companies may consider adopting the POLARIS approach and its outcomes as a reference for developing strategies to manage risks under varying ice conditions. Moreover, it is evident that high-resolution satellite imagery can significantly enhance navigational decision-making within ice-infested regions. Looking forward, there exists a necessity to conduct research at finer scales on operational risks in icy areas utilizing high spatial resolution satellite data. Additionally, given the relative ease and immediacy of temperature observations, it is essential to investigate the correlation between temperature and operational risks in icy waters and to explore its potential as a warning indicator.

5. Conclusions

This study effectively leveraged the POLARIS methodology to examine and quantify risks in seasonal ice zones, using the northern part of Liaodong Bay as a case study. The results, based on the mean RIO values and the proportion of days with RIO values below zero ($\text{RIO} < 0$), identified sectors 3, 4, 5, 7, 9, 10, and 11 in northern Liaodong Bay as areas of escalated risk, with sectors 5 and 10 displaying the utmost severity, whereas sectors 1 and 2 were relatively less risky. This analysis underscored a clear spatial disparity in operational risks between the western and eastern divisions of Liaodong Bay. The ratio of days with negative RIO values and the mean RIO value can serve as pragmatic tools for quantifying the degree of navigational risk in ice-infested waters, thereby enabling relevant government agencies and port/shipping companies to devise risk mitigation measures.

This study substantiated the potential of POLARIS in assessing operational risks in seasonal ice environments and delivered actionable insights that can guide authorities and enterprises in formulating more robust disaster prevention and mitigation strategies, thereby augmenting decision-making processes pertaining to vessel navigation in icy conditions. However, to ensure the successful implementation and practical application of POLARIS, it is essential to integrate its systematic evaluation techniques with the expert judgment and hands-on experience of mariners.

Author Contributions: J.X. and L.M. conceptualized this study; J.X. and S.X. carried out this study, performed the calculations, and drafted the paper; S.X., S.Q. and X.L. processed the review and editing of the paper. All authors have read and agreed to the published version of the manuscript.

Funding: This research was funded by the Program for Scientific Research Start-up Funds of Guangdong Ocean University: Research on the Navigability of Arctic Shipping Routes Based on Sea Ice Condition Analysis (Grant number: 060302132106), the Natural Science Foundation of Guangdong Province (Grant numbers: 2022A1515011603, 2023A1515011212), the Special Projects in Key Fields of Ordinary Universities in Guangdong Province (Grant numbers: 2021ZDZX1015, 2022ZDZX3005), the Natural Science Foundation of Shenzhen City (Grant numbers: JCYJ20220530162200001, JCYJ20210324122813036), the Program for Scientific Research Start-up Funds of Guangdong Ocean University (Grant number: 060302132009), and Postgraduate Education Innovation Project of Guangdong Ocean University (Grant numbers: 202421, 2023XSLT_032).

Institutional Review Board Statement: Not applicable.

Informed Consent Statement: Not applicable.

Data Availability Statement: The GF-4 satellite data can be downloaded from <https://data.cresda.cn/#/home> (accessed on 1 April 2022).

Conflicts of Interest: The authors declare no conflicts of interest.

References

1. Wang, M.; Wu, S.L.; Zheng, W.; Zhao, C.H.; Liu, C. Temporal-spatial distribution of Bohai Sea sea ice in long-time series and its correlation with air temperature. *Meteorol. Mon.* **2016**, *42*, 1237–1244.
2. Sun, J.Q.; Chen, X.J.; Li, Q.; Gao, J.Z.; Zhang, H.; Xu, Y.J. Temporal and Spatial Variation Characteristics of Sea Ice Conditions in the Bohai Sea from 1988 to 2018 Based on Remote Sensing Technology. *J. Catastrophol.* **2022**, *37*, 178–184+191.
3. Zheng, X.J.; Qiu, K.M.; Lu, F. Quantitative Calculation of Sea Ice over the Bohai Sea Using NOAA/AVHRR Imagery. *Q. J. Appl. Meteorol.* **1998**, *9*, 104–108.
4. Zhao, Q.H.; Wang, X.; Wang, X.F.; Li, Y. Temporal and Spatial Characteristics of Sea Ice Condition and Its Influencing Factors in Liaodong Bay from 2015 to 2020. *J. Geo-Inf. Sci.* **2021**, *23*, 2025–2041.
5. Ministry of Natural Resources, Marine Early Warning and Monitoring Bureau. *2021 China Ocean Disaster Bulletin*; Ministry of Natural Resources, Marine Early Warning and Monitoring Bureau: Beijing, China, 2022.
6. Fedi, L.; Etienne, L.; Faury, O.; Müller, R.P.; Stephenson, S.; Cheaitou, A. Arctic Navigation: Stakes, Benefits and Limits of the POLARIS System. *J. Ocean Technol.* **2018**, *13*, 54–67.
7. Kujala, P.; Kamarainen, J.; Suominen, M. Validation of the new risk-based design approaches (POLARIS) for Arctic and Antarctic operations. In Proceedings of the 25th International Conference on Port and Ocean Engineering under Arctic Conditions, Delft, The Netherlands, 9–13 June 2019.
8. Bond, J.; Hindley, R.; Kendrick, A.; Kmrinen, J.; Kuulila, L. Evaluating Risk and Determining Operational Limitations for Ships in Ice. In Proceedings of the 2018 Arctic Technology Conference, Houston, TX, USA, 5–7 November 2018.
9. Fedi, L.; Faury, O.; Etienne, L. Mapping and Analysis of Maritime Accidents in the Russian Arctic through the Lens of the Polar Code and POLARIS System. *Mar. Policy* **2020**, *118*, 103984. [[CrossRef](#)]
10. Tremblett, A.J.; Garvin, M.J.B.; Taylor, R.; Oldford, D. Preliminary Study on the Applicability of the POLARIS Methodology for Ships Operating in Lake Ice. In Proceedings of the 26th International Conference on Port and Ocean Engineering under Arctic Conditions, Moscow, Russia, 14–18 June 2021.
11. Moakler, E.; Bond, J.; Oldford, D.; Grant, M. Creation of Freshwater Ice POLARIS. In Proceedings of the 27th International Conference on Port and Ocean Engineering under Arctic Conditions, Glasgow, UK, 12–16 June 2023.
12. Qing, S. *Remote Sensing Research and Application of Salinity and Suspended Particle Size of the Bohai Sea*; Ocean University of China: Qingdao, China, 2011.
13. Pang, H. *Study on Spatial-Temporal Variation and the Relationship of Climatic Factors in Recent 50 Years in Bohai Sea*; Ludong University: Yantai, China, 2018.
14. Maritime Safety Committee. Appendix-Methodology for Assessing Operational Capabilities and Limitations in Ice: Polar Operational Limit Assessment Risk Indexing System (POLARIS). Available online: <https://www.imorules.com/GUID-2C1D86CB-5D58-490F-B4D4-46C057E1D102.html> (accessed on 1 March 2024).
15. Yuan, S. *The Space-Time Distribution of Sea Ice Resource Quantity in Bohai Sea and Its Response to Climate Change*; Beijing Normal University: Beijing, China, 2009.
16. Yuan, S.; Liu, C.; Liu, X. Practical Model of Sea Ice Thickness of Bohai Sea Based on MODIS Data. *Chin. Geogr. Sci.* **2018**, *28*, 863–872. [[CrossRef](#)]
17. Xie, F. *Preliminary Study on the Volume of Sea Ice Resources in the Bohai Sea*; Beijing Normal University: Beijing, China, 2003.
18. Shi, P.; Gu, W.; Xie, F.; Yuan, Y.; Ying, G.F. Spatial Characteristics of Sea Ice Resources of Liaodong Gulf in Winter. *Resour. Sci.* **2003**, *25*, 2–8.
19. Jin, B.Z. Entering Ice Regions: Commercial Operations and Safe Navigation. Available online: https://www.sohu.com/a/www.sohu.com/a/450698283_175033 (accessed on 2 March 2024).
20. Lou, Z.P.; Liu, J.L. Matters of Concern in Ice Navigation. *Shipping Transaction Gazette*, 26 January 2021.
21. Zhu, Y.Z. *Guidelines for Safe Operation of Ships in the Ice Area of Liaodong Bay and Northern Yellow Sea*; Dalian Maritime University Press: Dalian, China, 2015.
22. Wang, Y. [Risk Alert] Sea Ice in the Yellow and Bohai Seas Seriously Affecting Vessel Safety. Available online: https://www.sohu.com/a/www.sohu.com/a/220114740_175033 (accessed on 2 March 2024).
23. China Youth Online. Over 20% of the Sea Surface Covered by Ice: Liaodong Bay Sees Its Largest Ever Extent of Sea Ice at This Time of Year. Available online: <https://baijiahao.baidu.com/s?id=1785885355605401777&wfr=spider&for=pc> (accessed on 2 March 2024).
24. Zhang, R. Sea Ice Blue Alert Issued for the 12th Consecutive Time, Has the “Warm Winter” Reversed. Available online: <https://baijiahao.baidu.com/s?id=1789784462116628682&wfr=spider&for=pc> (accessed on 2 March 2024).

Disclaimer/Publisher’s Note: The statements, opinions and data contained in all publications are solely those of the individual author(s) and contributor(s) and not of MDPI and/or the editor(s). MDPI and/or the editor(s) disclaim responsibility for any injury to people or property resulting from any ideas, methods, instructions or products referred to in the content.